Proceedings of the 2014 22th International Conference on Nuclear Engineering
ICONE22
July 7-11, 2014, Prague, Czech Republic

ICONE22-30489

PREDICTION MODEL OF OXIDATION LAYER THICKNESS IN FLOW ACCELERATED CORROSION PROCESS

Ruixuan Han，Yi Peng, Huailin Li
State Nuclear Power Research Institute
Beijing，China

ABSTRACT

A new prediction model for the oxidation layer thickness of carbon steel is developed, that is based on the parabolic time law of corrosion and the mass transport balance theory. The relationship between the oxidation layer thickness and temperature, pH, and flow velocity is discussed. The predicted results show that the oxidation layer thickness increases exponentially with increasing temperature and decreases exponentially with increasing flow velocity. The oxidation layer thickness increases with increasing pH until pH=10.5 and then decreases. The predicted results agree with experimental results.

1. INTRODUCTION

In secondary circuit of nuclear power system, the failure of the carbon steel piping may come from flow accelerated corrosion (FAC). Since many serious accidents happened because of FAC, developing an accurate FAC model has attracted many interests in the past few decades. For example, a couple of models and prediction software of pipe wall thinning rates for FAC have been developed [1-6]. Sanchez-Caldera model[1] is a widely used prediction model. Although it is a simple model, it can be used to explain most important phenomena of FAC. The following formula can be used to described this model,

$$\frac{dm}{dt} = \frac{\theta \cdot \left(C_{eq} - C_{\infty}\right)}{1/k + (1-f)(1/K_d + \delta/D)} \quad (1)$$

Here m represents the thickness of the wall of the pipe. And dm/dt is the wall thinning rate in mol/(cm^2·s), C_{eq} represents the equilibrium concentration of Fe^{2+}/Fe^{3+} in mol/cm^3, which depends on temperature, hydrogen concentration, and pH; θ represents the porosity of open area in metal surface; K_d represents the mass transfer coefficient in cm/s; $k=A\exp(-E/RT)$ represents the reaction rate constant in cm/s; f represents the fraction of oxidized metal converted into magnetite at the metal-oxide interface, δ represents the oxidization layer thickness in cm, D denotes the diffusion coefficient of iron cations in water, C_{∞} represents the concentration of Fe^{2+}/Fe^{3+} in the bulk fluid in mol/cm^3.

The values of the parameters k, K_d, D and C_{eq} are roughly estimated. In the calculation procedure, the thickness of the oxidation layer used in Sanchez-Caldera model is 1 micron although the oxidation layer thickness ranges from 0.5 to 9 microns from experimental work [2]. However, the thickness of the oxidation layer is a function of temperature, pH, and other variables.

Experimental studies show that the oxidation layer thickness increases with the increasing pH value and increases with the decreasing fluid stream velocity. The oxidation layer thickness as a function of the pH and fluid velocity can be written as the following equation [7]:

$$\delta = \frac{\alpha pH}{U} \quad (2)$$

Where α is a constant, the pH is in the range of 8.0<pH<10.0 and U>0.

The fluid on the oxidation layer can generate internal stress inside the oxidation layer. Once the stress is greater than the ultimate strength of the oxidation layer, the oxidation is broken. Consequently, the thickness of the oxidation layer decreases. The oxidation layer thickness as a function of the pH value and the stress is given below:

$$\delta = \frac{apH}{e^{b\sigma_{\max}}} \quad (3)$$

Where a and b are constants, σ_{max} represents the maximum value of the Tresca stress of the oxidation layer in a certain velocity (kPa)[8].

The equations above for the thickness of the oxidation layer are all from experimental data. The temperature effect is ignored in these equations, but the temperature is very important for the oxidation layer growth. Several constants

in the equations are difficult to determine. In this paper, a calculation method is developed based on parabolic time law of corrosion and mass transport balance, which could overcome the disadvantages mentioned above.

2. OXIDATION LAYER THICKNESS CALCULATION MODEL

2.1 PARABOLIC TIME LAW AND OXIDATION LAYER THICKNESS CALCULATION MODEL

In autoclaves or flowing water loops with neutral and alkaline solutions, Potter and Mann [9] found that a duplex oxidation layer of carbon steel grows according to the parabolic law as follow:

$$\delta_0^2 = k_p t \tag{4}$$

Where δ_0 represents the thickness of the oxidation layer in still aqueous corrosion condition in m. t denotes the time in s, k_p represents the parabolic corrosion rate constant in m^2/s. This law fits for relatively thick oxidation layer and without pores.

The derivative of the thickness of the oxidation layer with respect to time is (5):

$$d\delta_0 / dt = k_p / 2\delta_0 \tag{5}$$

If fluid flows in a pipe, the mass transportation of soluble ferrous ions from the oxidation surface to the fluid flow will be significantly enhanced. Since the mass transport will reduce the thickness of the oxidation layer, the mass transportation process can be written as follow:

$$d\delta_u / dt = -K_d (C_{eq} - C_\infty) M / \rho \tag{6}$$

Where $d\delta_u/dt$ represents the change rate of oxidation layer thickness cased by in m/s; K_d represents the mass transfer coefficient from the oxidation layer surface to the main flow in m/s; C_{eq} represents equilibrium concentration of iron species in mol/cm^3); C_∞ represents the concentration of Fe^{2+}/Fe^{3+} in the bulk fluid (consider as 0) in mol/cm^3; M represents molar mass of iron (56 g/mol); ρ represents the density of iron (7.8 g/ cm^3).

The corrosion law in flow conditions should be same as that in still water. Therefore, the total oxidation layer thickness change rate in FAC condition can be expressed as:

$$\begin{aligned} d\delta / dt &= d\delta_0 / dt + d\delta_u / dt \\ &= k_p / 2\delta - K_d C_{eq} M / \rho \end{aligned} \tag{7}$$

When the system reaches equilibrium state, the thickness of oxidation layer is a constant:

$$d\delta / dt = 0 \tag{8}$$

So, the thickness of the oxidation layer at equilibrium state can be expressed as:

$$\delta = \frac{k_p \rho}{2 K_d C_{eq} M} \tag{9}$$

2.2 MASS TRANSFER COEFFICIENT

FAC rate is controlled by mass transfer, which includes two parts, the diffusion of Fe^{2+} in the corrosion reaction oxidation layer and the mass transfer from the boundary layer to main fluid. The mass transfer coefficient from boundary layer to main fluid is discussed here.

For the ensemble-averaged, steady, incompressible Navier-Stokes equations in Cartesian tensor notation can be written in the following form.

Continuity conservation equation:

$$\frac{\partial(\rho u_i)}{\partial x_i} = 0 \tag{10}$$

Momentum conservation equation:

$$\frac{\partial(\rho u_i u_j)}{\partial x_j} = -\frac{\partial p}{\partial x_i} + \frac{\partial}{\partial x_j}\left[\mu\left(\frac{\partial u_i}{\partial x_j} + \frac{\partial u_j}{\partial x_i}\right) + \tau_{ij}\right] \tag{11}$$

Energy conservation equation:

$$\frac{\partial(\rho u_i T)}{\partial x_i} = \frac{\partial}{\partial x_i}\left(\frac{\lambda}{c_p}\frac{\partial T}{\partial x_i}\right) \tag{12}$$

Where, ρ, u, p and T are density, velocity, pressure and temperature, respectively. And then μ, λ, and c_p represent laminar viscosity, thermal conductivity and specific heat. The time-averaged Reynolds stress tensor, τ_{ij}, is related to the utilization of turbulent model.

Regarding the mass transfer coefficient, Chilton-Colburn's analogy of heat and mass transfer is often used in a pipe with fully developed turbulence[10]. The mass transfer coefficient K_d in a straight pipe is obtained by using this analogy as:

$$K_d = \left(\frac{U_\tau}{U_m}\right)^2 \mathrm{Re} \cdot Sc^{1/3} \cdot \frac{D}{d} \tag{13}$$

Where U_τ is the friction velocity defined in reference [11]:

$$U_\tau = \sqrt{\nu\left[\frac{dU_m}{dy}\right]_{wall}} \tag{14}$$

And U_m is the mean velocity, Re is the Reynolds number, Sc is the Schmidt number, d is the hydraulic diameter, v is the kinematic viscosity, and D is the diffusion coefficient of Fe^{2+} in water.

$$D = 2.5 \times 10^{-15} T / \mu_e \tag{15}$$

Substituting the definition formula of Re and Sc into equation (13), we have the following equation for K_d:

$$K_d = \frac{\tau}{U_m \rho}\left(\frac{\mu}{\rho \cdot D}\right)^{-2/3} \tag{16}$$

The shear stress can be written as:

$$\tau = \mu_e \frac{U_s}{X_s} \quad (17)$$

Where μ_e is effective viscosity, which could estimated by equation (18).

$$\mu_e = 0.00179(1 + 0.3368t + 0.000221t^2)^{-1} \quad (18)$$

U_s is velocity of the first node from wall, and X_s is the distance of the first node from wall.

2.3 SOLUBILITY OF FE^{2+}

With low oxygen concentration, the oxidation layer of iron mainly contains magnetite and the chemical formula is Fe_3O_4. The Fe_3O_4 layer dissolves in the water and the chemical reaction for this process can be written as [12]:

$$Fe_3O_4 + (2\text{-}x)H^+ + \frac{1}{3}H_2 \rightleftharpoons Fe(OH)_x^{2-x} + (\frac{4}{3}\text{-}x)H_2O \quad (19)$$

x=0, 1, 2, 3

The reaction equilibrium constants of the above equations are K_0, K_1, K_2, and K_3, respectively. Then, K_x is represented by the following:

$$K_x = \frac{Fe(OH)_x^{(2-x)+}}{\left[H^+\right]^{(2-x)}\left[H_2\right]^{1/3}} \quad (20)$$

where x is equal to 0, 1, 2, and 3, respectively.

The equilibrium constant is calculated as follows:

$$\ln K_x = -\frac{A}{RT} + \frac{B}{R}(\ln T - 1) + \frac{C}{R} \quad (21)$$

The values of parameters A, B, and C are listed in Table 1.

Table 1. Values of the parameter A, B, and C

Corrosion product	A (J/mol)	B (J/mol/K)	C (J/mol/K)
Fe^{2+}	-112449	41	-340
$FeOH^+$	-49091	14	-179
$Fe(OH)_2$	19309	0	-99
$Fe(OH)^{3-}$	37844	0	-207

The concentration of iron C_{eq} is calculated as follow:

$$\begin{aligned} C_{eq} &= \left[Fe^{2+}\right] + \left[FeOH^+\right] + \left[Fe(OH)_2\right] + \left[HFeO_2^-\right] \\ &= \left\{K_0\left[H^+\right]^2 + K_1\left[H^+\right] + K_2 + \frac{K_3}{\left[H^+\right]}\right\}\left[H_2\right]^{1/3} \\ &= \left\{K_0 10^{-2pH} + K_1 10^{-pH} + K_2 + K_3 10^{pH}\right\}\left[H_2\right]^{1/3} \end{aligned} \quad (22)$$

The concentration of H_2 is in the range from 0.00078 to 0.00325 mol/L[13]. The concentration taken in this work is 0.001 mol/L.

Ammonia is a typical chemical agent used for the pH control in the feed water system of power plants. The pH value is influenced by the concentration and the hydrolysis degree of NH_3. And the hydrolysis degree is a function of temperature. The temperature effect on the pH value is evaluated base on those thinking . The hydrolysis constant of NH_3, K_{NH3}, as a function of temperature can be obtained from reference [14]. The temperature dependence of ionic product of water, K_w, was calculated, according to reference [15]:

$$NH_3 + H_2O \rightleftharpoons NH_4^+ + OH^- \quad (23)$$

$$K_{NH_3} = \frac{\left[NH_4^+\right]\left[OH\right]^-}{\left[NH_{3,aq}\right]} \quad (24)$$

The degree of hydrolysis of ammonia is calculated by equation (25):

$$\alpha = \frac{K_{NH_3}}{K_{NH_3} + \frac{K_w}{\left[H^+\right]}} \quad (25)$$

The Ammonia concentration is calculated by equation (26):

$$C = \frac{K_w - \left[H^+\right]^2}{\alpha\left[H^+\right]} \quad (26)$$

Replace α in equation (26) with right side of equation (25):

$$\begin{aligned} &K_{NH_3}\left[H^+\right]^3 + \left(K_w + K_{NH_3}C\right)\left[H^+\right]^2 \\ &-K_wK_{NH_3}\left[H^+\right] = K_w^2 \end{aligned} \quad (27)$$

The H^+ concentration of the solution at different temperatures can be obtained by substituting the values of K_{NH3}, K_w and C at this temperature. And then pH can be caculated.

2.4 PARABOLIC RATE CONSTANT OF CARBON STEEL IN AQUEOUS

J. Roberson[16] has reported the relation between pH value and the parabolic rate constants k_p of iron. The k_p roughly increases with $(pH)^2$ linearly in the high pH range ($[OH^-]$>0.1mol/L). In the lower pH values region ($[H^+]<10^{-5}$ mol/L and $[OH^-]$<0.01mol/L), the k_p is independent of pH. In the region $[H^+]>10^{-4}$ mol/L, k_p is independent of time. The water chemistry of nuclear power plant is in a mild alkaline condition, which means the k_p could be simply considered independent of pH.

Based on the experimental data of carbon steel in neutral water by M. Warzee [17, 18], k_p as a function of temperature (<350°C) can be written as:

$$\log k_p = \frac{-2701}{T} - 14.33 \quad (m^2/s) \quad (28)$$

In summary, the oxidation layer thickness can be expressed as follow:

$$\delta = \frac{10^{-2701/T-14.33}}{\frac{2\tau}{U_m\rho}\left(\frac{\mu}{\rho\cdot D}\right)^{-2/3}\cdot\left\{K_0 10^{-2\mathrm{pH}}+K_1 10^{-\mathrm{pH}}+K_2+K_3 10^{\mathrm{pH}}\right\}\left[\mathrm{H}_2\right]^{1/3}} \quad (29)$$

(5<pH<12, T<350°C)

3. RESULTS AND DISCUSSION

3.1 MASS TRANSFER COEFFICIENT

The mass transfer coefficient as a function of temperature is shown in Figure 1A. As temperature increased, the mass transfer coefficient increases exponentially, which indicates that if the temperature is increased, the mass transfer will be faster. Equation (14-16) shows that as temperature increasing, the viscosity decreases exponentially and the mass transfer coefficient increased. Flow velocity effect on the mass transfer coefficient is shown in Figure 1B. As flow velocity increasing, mass transfer coefficient increases linearly. Those results are consistent with previous work [3, 7].

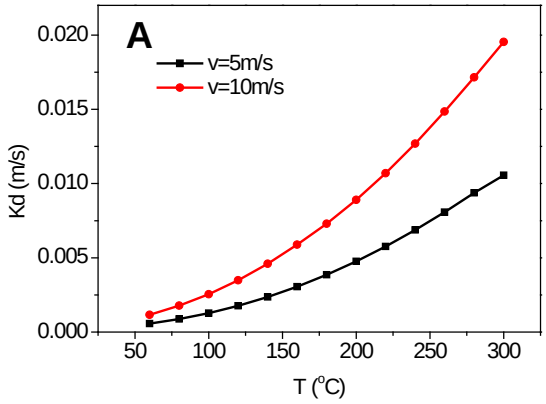

Figure 1A. Mass transfer coefficient as a function of temperature .

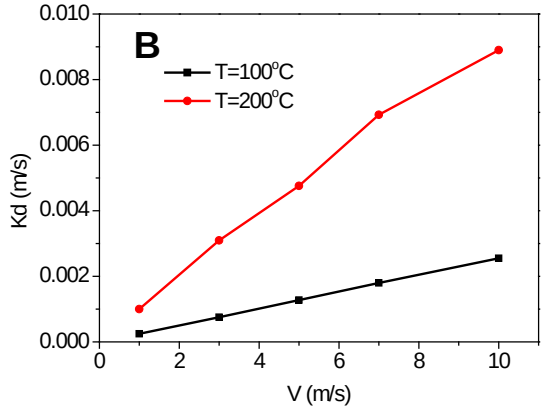

Figure 1B. Mass transfer coefficient as a function of flow velocity .

3.2 SOLUBILITY OF MAGNETITE

The solubility of magnetite as a function of pH value and temperature is shown in Figure 2, which is calculated via equation (22). In Figure 2A, the solubility of magnetite increases with the increasing temperature in low temperature region 80~100°C. After that, the solubility of the magnetite decreases with the increasing temperature. This result agrees with Zhong's work [7]. In Figure 2B, magnetite solubility decreases with increasing pH value until pH=10.5. When pH larger than 10.5, the solubility of magnetite increases with increasing pH value. Besides, when pH is lower than 9.7, higher temperature lowers the solubility of Fe_3O_4. When pH is higher than 9.7, higher temperature increases the solubility of Fe_3O_4.

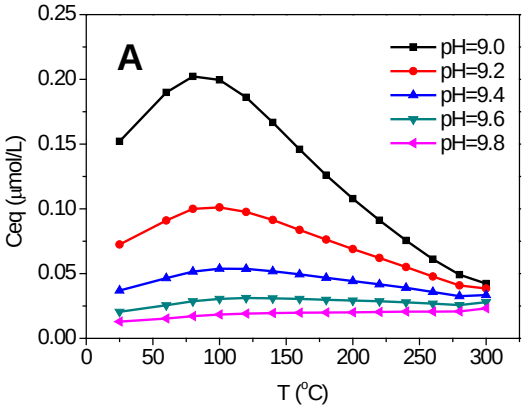

Figure 2A. The solubility of magnetite as a function of temperature in different pH environments.

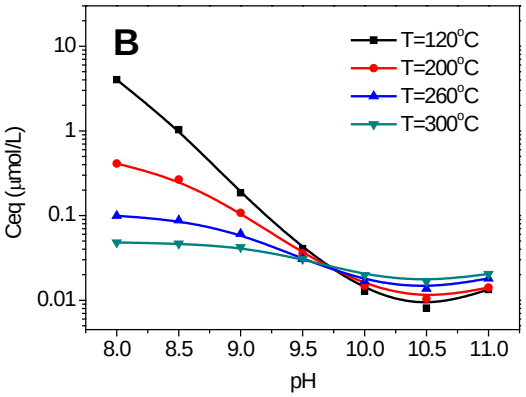

Figure 2B. The solubility of magnetite as a function of pH value under different temperature condition.

3.3 TEMPERATURE, PH VALUE, AND FLOW VELOCITY EFFECTS ON THE OXIDATION LAYER THICKNESS

Temperature, pH value, and flow velocity affect the thickness of the the oxidation layer. The relationship between the oxidation layer thickness and temperature is shown in Figure 3A. In this figure, the oxidation layer thickness increases with increasing temperature exponentially. When the temperature is lower than a critical temperature value, the oxidation layer thickness is very low. When the temperature is larger than the critical value, the oxidation layer thickness increases with increasing temperature dramatically. The

critical temperature value reduced from 150°C to 80 °C with increasing pH value from 9.0 to 9.8.

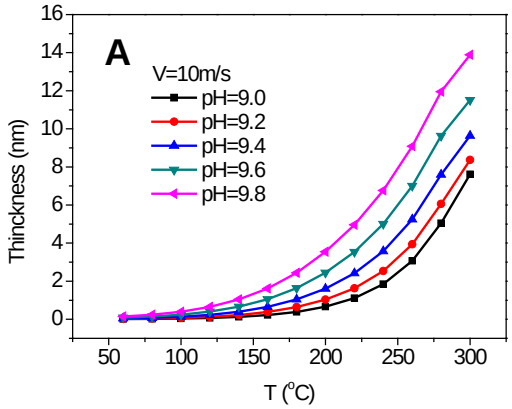

Figure 3A. The oxidation layer thickness as a function of temperature under different pH condition.

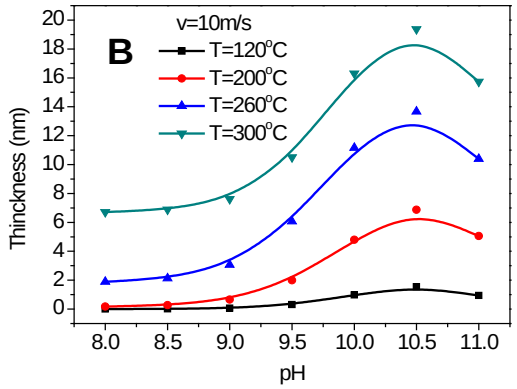

Figure 3B. The oxidation layer thickness as a function of pH value at different temperature.

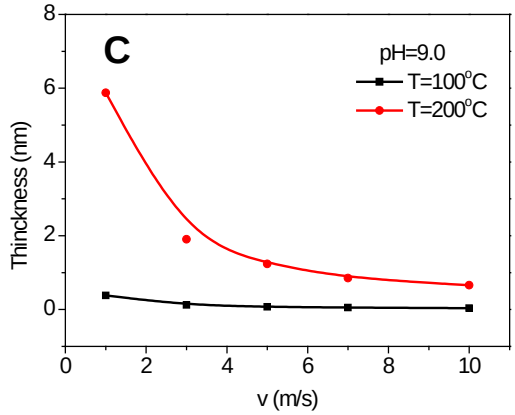

Figure 3C. The oxidation layer thickness as a function of the flow velocity at different temperature.

From Figure 3B, oxidation layer thickness increases with increasing pH value until pH=10.5. After that, the thickness decreased. In the range of pH=8.0~10.0, the oxidation layer thickness increases with increasing pH value exponentially, rather than increases linearly as predicted by equation (2-3). The oxidation layer thickness decreases above pH=10.5 because the magnetite solubility increases as showed in Figure 2B.

The relationship between the flow velocity and temperature is shown in Figure 3C. The oxidation layer thickness decreases exponentially with increasing flow velocity. This trend is different from equation (2), which shows a linear relation but this trend agrees with equation (3).

Bouchacourt and Remy's experimental results show that when the pH(at room temperature)=9.0, the oxidation layer is very thin at 75°C, while the oxidation layer becomes around 1 micro at 125°C, 180°C and 225°C, but the oxidation layer becomes porous structure at 125°C, the oxidation layer structures formed at 180°C and 225 °C are more compact [7]. In this work, pores are not considered in the growing oxidation layer . So the porous oxidation layer is ignored. It is predicted that under condition pH=9.0 the oxidation layer thickness decreases rapidly above 150°C which is consistent with the trend of the experimental results. However, the thickness value predicted is much lower than 1 micro in the experiment. There are two main reasons. One is the velocity effect on the oxidation layer thickness. The other is that the pores effect on the corrosion rate.

4. CONCLUSIONS

In this paper, a new prediction model for the oxidation layer thickness of carbon steel is developed, that is based on the parabolic law of corrosion and the mass transport balance theory. The relationship between the oxidation layer thickness and temperature, pH value, and flow velocity is discussed. The conclusions are presented below.

The oxidation layer thickness increases exponentially with increasing temperature and decreases exponentially with increasing flow velocity. The oxidation layer thickness increases with increasing pH until pH=10.5 and then decreases. The predicted results agree with experimental results.

This oxidation layer thickness prediction model based on the parabolic law and the mass transport balance theory offer a more accurate relationship between thickness and temperature, pH value, and velocity. The application scope of pH is extended from 8~10 to 5~12 (all at room temperature). And it doesn't include uncertain constants which can be applied more easily. The pores structure is ignored in this model. As a result, this model cannot predict the thickness of oxidation layer with porous.

ACKNOWLEDGMENTS

We acknowledge Dr. Xueyuan Zhang and Dr. Wei Xiao for valuable comments and discussion. This work is supported by innovation project of State Nuclear Power Technology Corporation .

REFERENCES

1. Sanchez-Caldera, L.E., *The Mechanism of corrosion-Erosion in steam extraction lines of power stations*, in *Mechaical Engineering*1984, Massachusets institute of Technology.

2. Betova, I., M. Bojinov, and T. Saario, *Predictive modelling of flow-accelerated corrosion – unresolved problems and issues*, 2010, Technical Research Center of Finland: Finland. p. 53.
3. Abdulsalam, M. and J. Stanley, *Steady-State Model for Erosion-Corrosion of Feedwater Piping.* Corrosion, 1992. **48**(7): p. 587-593.
4. Ardillon, E., B. Villain, and M. Bouchacourt. *Probabilistic Analysis of Flow-Accelerated Corrosion in French PWR: the Probabilistic Module of BRTCICERO, Version 2.* in *7th International Conference on Structural Safety and Reliability (ICOSSAR 97),*. 1997. Kyoto, Japan,November 24-28, 1997.
5. Kanster, W., et al., *Calculation code for erosion corrosion induced wall thinning in piping system.* Nucl. Eng. Des., 1990. **119**: p. 431-438.
6. Guo, H., B. Lu, and J. Luo, *Non-Faraday material loss in flowing corrosive solution.* Electrochimica acta, 2006. **51**(25): p. 5341-5348.
7. Zhong, L., L. Chun-bo, and Z. Yu-gui, *Numerical Simulation of Flow-Accelerated-Corrosion of Carbon Steel in Single Liquid Phase Flow.* Nuclear Power Engineering, 2009. **30**(5): p. 48-53.
8. Zhu, X.L., et al., *A novel method to determine flow-accelerated corrosion rate based on fluid structure interaction.* Materials and Corrosion, 2013: p. n/a-n/a.
9. Potter, E.C. and G.M.W. Mann, *Oxidation of Mild Steel in High- Temperature Aqueous System*, in *1st Int. Congress on Metallic*1961.
10. Chilton, T.H. and A.P. Colburn, *Mass transfer (absorption) coefficients prediction from data on heat transfer and fluid friction.* . Industrial & engineering chemistry, 1934. **26**(11): p. 1183-1187.
11. Nishiguchi, I., et al., *A review: Japanese pipe wall thinning management based on JSME rules recent R&D studies performed to enhance the rules.* J. Adv. Mainten, 2010. **2**: p. 14-24.
12. Sweeton, F.H. and C.F. Baes Jr, *The solubility of magnetite and hydrolysis of ferrous ion in aqueous solutions at elevated temperatures.* The Journal of Chemical Thermodynamics, 1970. **2**(4): p. 479-500.
13. Zhu, X.L., X.F. Lu, and X. Ling, *A novel method to determine the flow accelerated corrosion rate in the elbow.* Materials and Corrosion, 2013. **64**(6): p. 486-492.
14. Han, Y., *pH Control of Primer and Secondary Loop of Nuclear Power Plants*, in *Water Chemistry of Nuclear Power Plants*. 2010: Beijing. p. 178.
15. *Release on the Ionization Constant of H2O*. The International Association for the Properties of Water and Steam 2007; Available from: http://www.iapws.org/relguide/Ionization.pdf.
16. Robertson, J., *The mechanism of high temperature aqueous corrosion of steel.* Corrosion Science, 1989. **29**(11–12): p. 1275-1291.
17. Warzee, M., C. Sonnen, and P. Berge, 1967, EURAEC Report.
18. Robertson, J., *The mechanism of high temperature aqueous corrosion of stainless steels.* Corrosion Science, 1991. **32**(4): p. 443-465.